Fat Suppressed Contrast-Enhanced T1-Weighted Dynamic Magnetic Resonance Imaging at 3T: Comparison of Image Quality Between Spectrally Adiabatic Iversion Recovery and the Multiecho Dixon Technique in Imaging of the Prostate

Yuji Iyama, MD,*†‡ Takeshi Nakaura, MD, PhD,*† Masafumi Kidoh, MD,† Kazuhiro Katahira, MD, PhD,‡ Tomohiro Namimoto, MD, PhD,† Shoji Morishita, MD,‡ and Yasuyuki Yamashita, PhD†

Objective: To compare the quality of fat suppression and image quality between multiecho Dixon technique (mDixon) and spectrally adiabatic iversion recovery (SPAIR) in dynamic contrast-enhanced magnetic resonance imaging of the prostate.

Methods: This prospective study assigned thirty consecutive patients to scanning with SPAIR technique (SPAIR protocol) and another consecutive 30 patients to scanning with mDixon technique (mDixon protocol). We calculated the contrast, signal to noise ratio (SNR), contrast to noise ratio (CNR) and the coefficient of variation between the 2 protocols. Two readers compared homogeneity of fat suppression, image noise, image contrast, and image sharpness between the two protocols.

Results: The SNR, CNR, and contrast of mDixon protocol were significantly higher than those of the SPAIR protocol (SNR: 14.7 ± 4.1 vs 11.0 ± 2.6; $P < 0.05$; CNR: 6.3 ± 1.6 vs 0.5 ± 1.5; $P < 0.01$; contrast: 4.4 ± 1.4 vs 1.3 ± 0.5; $P < 0.01$), whereas the coefficient of variation of mDixon protocol was significantly lower than that of SPAIR protocol (34.7 ± 15.5 vs 43.7 ± 23.1, $P < 0.01$). In qualitative image analysis, the image scores for the homogeneity of fat suppression, image noise, and image sharpness were significantly higher with mDixon protocol than those with SPAIR protocol ($P < 0.01$). There was no significant difference in image contrast between 2 fat suppression protocols ($P > 0.05$).

Conclusions: In dynamic contrast-enhanced magnetic resonance imaging of the prostate, mDixon technique improved the homogeneity of fat suppression without degrade of image quality compared with SPAIR technique.

Key Words: magnetic resonance imaging, prostate MRI, fat suppression techniques

The clinical utility of magnetic resonance imaging (MRI) to detect prostate carcinoma is well documented.[1–3] Among MRI systems, the signal-to-noise ratio (SNR) of 3T scanners is theoretically 2 times better than that of comparable 1.5T

scanners.[4] Additionally, contrast enhancement of 3T MRI is significantly higher than that of 1.5T MRI.[5] In dynamic enhanced prostatic MRI, the use of 3T MRI was shown to improve temporal and spatial resolution.[6,7] However, in 3T MRI systems, there is a technical challenge in suppressing fat signals despite the use of fat suppression techniques such as chemical shift selective fat suppression (CHESS),[8] because 3T MRI yields the relatively larger inhomogeneity of the magnetic field compared with 1.5T MRI.[9]

Dynamic MRI provides increased accuracy in localizing prostatic cancer.[10–12] Extracapsular tumor extension might be unclear in dynamic prostatic MRI without fat-suppression technique, because prostate was surrounded by periprostatic fat. Therefore, in clinical prostatic MRI, fat suppression technique might be useful to detect of extracapsular tumor extension.[13–16] The CHESS technique has been mostly used for fat suppression. However, this technique may lead to heterogeneous fat suppression[17] because of magnetic field inhomogeneity. Spectrally selective adiabatic inversion recovery (SPAIR) and multiecho Dixon (mDixon) imaging overcome these disadvantages of fat suppression technique in dynamic enhanced 3T MRI.[18–20] Spectrally selective adiabatic inversion recovery is a hybrid technique combining features of both CHESS and short TI inversion recovery (STIR)[21] with adiabatic pulses.[22] It is relatively insensitive to magnetic field inhomogeneity and, unlike CHESS, allows homogeneous fat suppression. On the other hand, the mDixon technique offers both flexibility in the choice of echo time and strong phase correction.[23] It is also less sensitive than CHESS with respect to magnetic field inhomogeneity. However, the 2 technique have yet to be compared to determine which is better-suited in dynamic enhanced 3T MRI of the prostate.

Therefore, the purpose of this study was to compare the image quality obtained from the SPAIR and the mDixon technique in dynamic contrast-enhanced MRI of the prostate.

MATERIALS AND METHODS

This prospective study was approved by our institutional review board. Prior informed consent to participate in the study was obtained from all patients.

Patients

Between July 2012 and August 2013, 60 consecutively registered patients underwent dynamic contrast-enhanced MRI for the detection of prostate cancer.

Body weight (BW), height, body mass index (BMI) and age were recorded. We also obtained BW measurements for all patients before the MRI examinations to allow us to tailor the amount of contrast medium administered. Patients suspected of

TABLE 1. Magnetic Resonance Imaging Sequence and Parameters

Sequence	m-Dixon-eTHRIVE	SPAIR-eTHRIVE
TR, ms	4.5	4.8
TE, ms	TE1, 1.51 TE2, 2.7	2.4
Slice thickness, mm	1	1
Interslice gap, mm	0	0
Flip angle, degrees	10	10
Matrix	172×268	256×219
FOV, mm	200×200	200×200
No. slices	100	100
Slice orientation	Axial	Axial
Voxel size, mm^3	$0.63 \times 0.63 \times 1.0$	$0.69 \times 0.69 \times 1.0$
No. acquisitions	1	1
Band width, Hz	1101.1	393.8
Mean acquisition time, s	145.2	151

FOV indicates field of view.

having prostate cancer based on a prostate-specific antigen level greater than 4.0 ng/mL were included. There were no excluded patients in this study. Consequently, all 60 patients (age range, 45–87 years; mean age, 56 years) satisfied the inclusion criteria.

MRI Examinations

All MRIs were acquired using a 3T whole-body MR system (Ingenia, Philips Medical Systems, Best, The Netherlands) equipped with a dual-source parallel radiofrequency transmission system in which a 32-channel phased-array coil served as the receiver coil. Patients were placed in the supine position with their arms raised. The following sequences were acquired: T2-weighted (T2w) 2-dimensional turbo-spin echo imaging, T2w volumetric isotropic turbo spin echo acquisition imaging, T1-weighted (T1w) 2-dimensional turbo-spin echo imaging, diffusion weighted imaging, T1w 3D turbo-field-echo sequence for dynamic enhanced MRI with fat suppression techniques (SPAIR or mDixon). Table 1 shows the parameter of T1w 3D turbo-field-echo sequence for dynamic enhanced MRI with fat suppression techniques.

Dynamic images were scanned from the apex to the base of the prostate, acquiring 100 slices. A dynamic series consisted of a precontrast series followed by a four-phase postcontrast series with enhanced-T1 high-resolution isotropic volume examination (eTHRIVE) (Philips Healthcare, Best, The Netherlands). Consecutive thirty patients were assigned to scanning using eTHRIVE with SPAIR technique (SPAIR-eTHRIVE) and another consecutive 30 patients using eTHRIVE with mDixon technique (mDixon-eTHRIVE). Default settings and the same imaging parameters for the two sequences were used as often as possible. Nonetheless, some parameters differed because of instrument-related restrictions and the sequences provided by the vendor.

Postcontrast series were obtained from patients injected with an adjusted amount (0.1 mmol/kg) of gadopentetate dimeglumine (Magnevist; Schering, Berlin, Germany) at a rate of 2 mL/s via an automatic injector, followed by 20 mL flush of saline.

Dynamic MRI of the prostate was carried out using a fixed time-delay method. After the precontrast series, gadopentetate dimeglumine was injected within 10 seconds. Postcontrast series (first, second, third, and fourth phases) were obtained 20, 50, 80, and 110 seconds after the initiation of contrast-agent injection. All scans were sent to picture archiving and communication system (PACS; Synapse: Fujifilm, Tokyo, Japan).

Quantitative Image Analysis

A radiologist who was blinded to the protocols with 5 years of experience in MRI of the prostate recorded the data from the axial source images of second phase. The reason why we selected the second phase was that second phase image was arterial phase image in our institution. The usefulness of evaluation of arterial phase image for diagnosis of prostate cancer was previously reported.[24] Therefore, we selected the arterial phase image in evaluation of quantitative image analysis. Six regions of interest (ROIs) were placed on the bilateral subcutaneous fat in the abdominal and buttocks and bilateral perirectal fat. The mean signal intensities of the 6 ROIs were recorded (ROI$_{Fa}$). Signal intensity was set to allow the selection of an ROI of 100 mm^2 in the subcutaneous fat, avoiding muscle. Additionally, 2 ROIs were placed on the bilateral prostatic transition zone at the level of mid gland, and the mean signal intensity of the 2 ROIs (ROI$_{Pro}$) were recorded. Signal intensity was set to allow the selection of an ROI of 50 to 100 mm^2 in the prostatic transition zone, avoiding periprostatic fat and prostatic peripheral zone. Figure 1 showed the demonstrating where regions of interests (ROIs) were placed. Contrasts were calculated as follows: ROI$_{Pro}$/ROI$_{Fat}$. The SNR was calculated as follows: ROI$_{Pro}$/SD of the ROI$_{Pro}$. The contrast-to-noise ratio (CNR) was calculated as previously reported[25]: (ROI$_{Pro}$ − ROI$_{fat}$)/[(SD of the ROI$_{Pro}$)^2 + (SD of the ROI$_{Fat}$)^2]$^{1/2}$. To measure the homogeneity of fat suppression, a coefficient of variation (CV), defined as the SD divided by the mean of the 6-point ROI$_{Fa}$, was calculated as previously reported.[26] We compared contrast, SNR, CNR, and CV of the 2 fat suppression protocols.

Qualitative Image Analysis

To determine the better of 2 fat suppression techniques, 2 board-certified urological radiologists who were blinded to the protocols with 7 and 5 years of experience in prostate MRI independently reviewed the images.
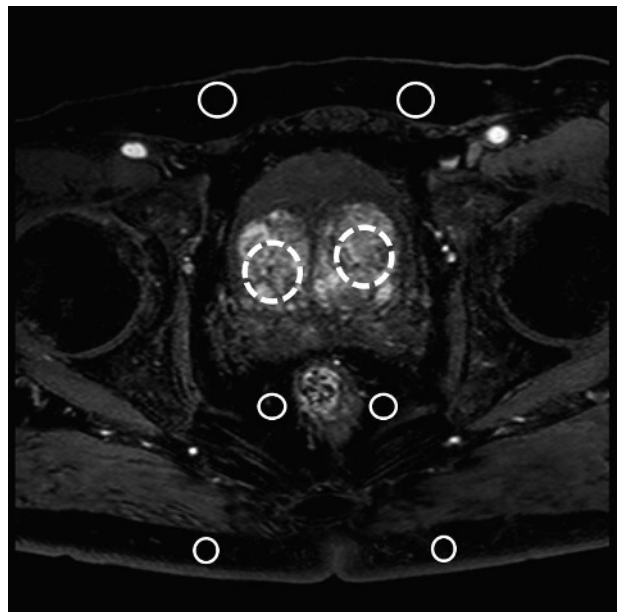
FIGURE 1. Demonstrating where ROIs were placed. Six ROIs were placed on the bilateral subcutaneous fat in the abdominal and buttocks, and bilateral perirectal fat (solid outlined circles). Additionally, 2 ROIs were placed on the bilateral prostatic transition zone at the level of mid gland (dotted outlined circles).

The radiologists retrospectively reviewed the first and second phase's images in mDixon-eTHRIVE or SPAIR-eTHRIVE. The images were reviewed subjectively regarding the homogeneity of fat suppression, image noise, image contrast, and the image sharpness of the prostate margin.

The radiologists used a four-point scale to evaluate the homogeneity of fat suppression, image contrast, image noise, and image sharpness. They scored image contrast considering the enhancement quality of femoral artery. They used the first and second phase's images to evaluate femoral arterial enhancement and score the image contrast strictly. They scored the homogeneity of fat suppression considering fat suppression of subcutaneous fat and perirectal fat. The homogeneity of fat suppression and image contrast were scored as follows, (1, unacceptable; 2, acceptable; 3, good; 4, excellent). Additionally, image noise was scored as follows, (1, so much image noise and clinically unacceptable; 2, image noise present and interfering with evaluation of adjacent structures; 3, image noise present but not interfering with evaluation of adjacent structures; 4, minimal or no noise). Image sharpness was assessed by evaluating sharpness of prostatic capsule and scored as follows, (1, blurry and readers cannot evaluate the border of prostatic capsule; 2, poorer than average; 3, better than average; 4, sharpest). They evaluated the homogeneity of fat suppression, image noise, and image sharpness of the prostate margin, using the second phase's images.

Statistical Analysis

All numeric values are reported as means ± SDs. Data were tested for normality using the Kolmogorov-Smirnov test. The age, BW, height, BMI, CNRs, SNR, contrasts, and CV are indicated normality. Therefore, we compare the age and BW, height, BMI of the patients, CNRs, SNR, contrasts, and CV of the images between mDixon-eTHRIVE and SPAIR-eTHRIVE protocols, using an unpaired 2-tailed Student t test. The visual scores assigned to the 2 sets of images were compared using the Mann-Whitney U test. P value less than 0.05 was considered statistically significant.

We evaluated the scale for the kappa coefficients using the free statistical software "R." We categorized interobserver agreement as follows, (<0.20, poor; 0.21–0.40, fair; 0.41–0.60, moderate; 0.61–0.80, substantial; and 0.81–1.00, near-perfect) (R package version 2.6.1; The; http://www.r-project.org/).

RESULTS

Patient Characteristics

There were no significant differences between mDixon-eTHRIVE group and SPAIR-eTHRIVE group with respect to age, BW, height, and BMI (age: 68.2 ± 11.7 vs 67.3 ± 10.5, P = 0.55; BW: 60.7 ± 12.0 kg vs 59.2 ± 10.8 kg, P = 0.60; height: 1.68 ± 0.06 m vs 1.65 ± 0.06 m, P = 0.10; BMI: 22.6 ± 2.2 kg/m^2 vs 22.0 ± 3.0 kg/m^2, P = 0.20).

TABLE 2. Quantitative Image Analysis

Parameter	SPAIR-eTHRIVE	mDixon-eTHRIVE	*P*
Image contrast	1.3 ± 0.5	4.4 ± 1.4	<0.01
SNR	11.0 ± 2.6	14.7 ± 4.1	<0.05
CNR	0.5 ± 1.5	6.3 ± 1.6	<0.01
CV	43.7 ± 23.1	34.7 ± 15.5	<0.01

Unless otherwise indicated, data are mean ± SD.

TABLE 3A. Qualitative Image Analysis (Reader 1) (Re: Reviewer 4)

Parameter	SPAIR-eTHRIVE	mDixon-eTHRIVE	*P*
Homogeneity of fat suppression	2.5 ± 0.8	3.4 ± 0.8	<0.01
Image noise	2.7 ± 0.9	3.2 ± 0.7	<0.01
Image contrast	3.5 ± 0.8	3.9 ± 0.3	0.06
Image sharpness	3.2 ± 0.7	3.5 ± 0.7	0.04

Unless otherwise indicated, data are mean ± SD.

Quantitative Image Analysis

Table 2 summarized the results of the quantitative image analysis. The SNR, CNR, and the contrast of the mDixon-eTHRIVE protocol were higher than those of the SPAIR-eTHRIVE protocol (CNR and contrast; P <0.01, SNR; P <0.05). The CV of the mDixon-eTHRIVE protocol was significantly lower than that of the SPAIR-eTHRIVE protocol (P <0.01).

Qualitative Image Analysis

Tables 3A and 3B summarized the results of the qualitative image analysis. The mean scores of homogeneous fat suppression, image noise, and image sharpness for the mDixon-eTHRIVE protocol were significantly higher than those for the SPAIR-eTHRIVE protocol (homogeneous fat suppression: reader 1, 3.4 ± 0.8 vs 2.5 ± 0.8, P < 0.01; reader 2, 3.2 ± 0.8 vs 2.4 ± 0.8, P < 0.01; image noise: reader 1, 3.2 ± 0.7 vs 2.7 ± 0.9, P < 0.01; reader 2, 3.2 ± 0.6 vs 2.6 ± 0.7, P < 0.01; and image sharpness: reader 1, 3.5 ± 0.7 vs 3.2 ± 0.7, P =0.04; reader 2, 3.5 ± 0.7 vs 2.9 ± 0.5, P < 0.01). There was no significant difference in image contrast between the mDixon-eTHRIVE and SPAIR-eTHRIVE protocols (reader 1: 3.9 ± 0.3 vs 3.5 ± 0.8, P = 0.06; reader 2, 3.9 ± 0.3 vs 3.7 ± 0.6, P = 0.20) (Tables 3A and 3B). Interobserver agreement regarding the homogeneity of fat suppression, image noise, image contrast, and image sharpness was moderate to substantial (κ = 0.71, 0.77, 0.76, and 0.81, respectively). Representative cases are shown in Figures 2 and 3.

DISCUSSION

Dynamic enhanced 3T MRI of the prostate using the mDixon technique resulted in stronger homogeneous suppression of the fat signal and higher image quality than obtained with the SPAIR technique.

Spectrally adiabatic iversion recovery is a variant of the spectral presatuation with inversion recovery method, which combines features of the CHESS and STIR techniques.[21,22] Like STIR, the spectral presatuation with inversion recovery technique uses inversion pulses for the preparatory module that can be appended to other sequences. These inversion pulses were designed

TABLE 3B. Qualitative Image Analysis (Reader 2) (Re: Reviewer 4)

Parameter	SPAIR-eTHRIVE	mDixon-eTHRIVE	*P*
Homogeneity of fat suppression	2.4 ± 0.8	3.2 ± 0.8	<0.01
Image noise	2.6 ± 0.7	3.2 ± 0.6	<0.01
Image contrast	3.7 ± 0.6	3.9 ± 0.3	0.2
Image sharpness	2.9 ± 0.5	3.5 ± 0.7	<0.01

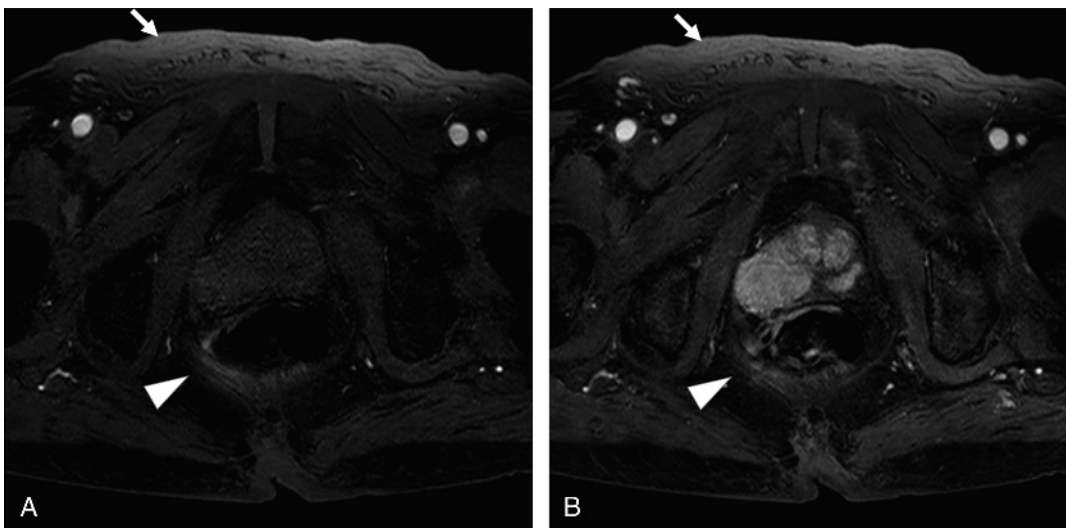Unless otherwise indicated, data are mean ± SD.
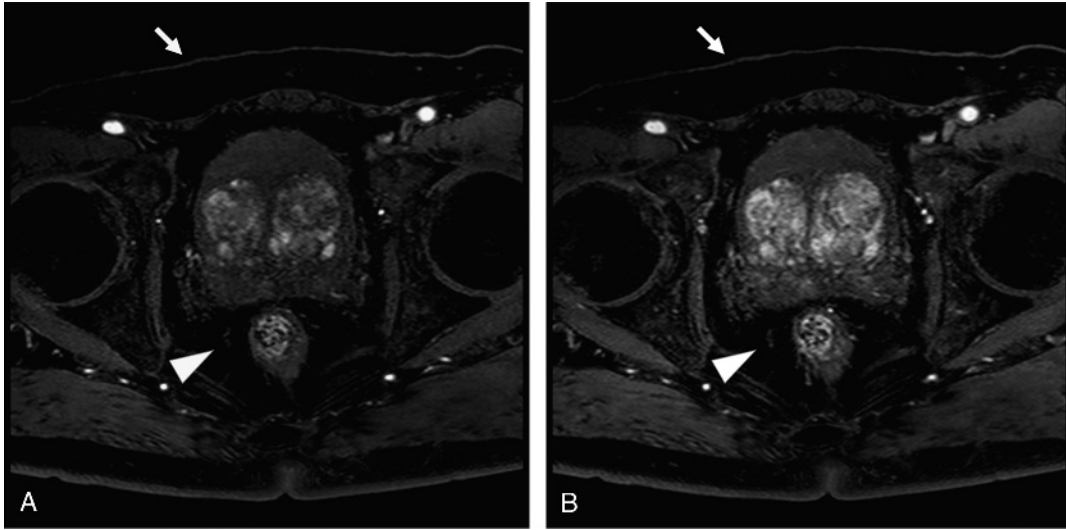
FIGURE 2. A 71-year-old man weighing 61 kg was suspected of having prostate carcinoma based on an elevated prostate-specific antigen level. He was underwent dynamic enhanced 3T MRI of the prostate with mDixon technique. The signal intensity of subcutaneous fat (arrows) and perirectal fat (arrowheads) are suppressed by mDixon technique in first phase image and second phase image (A and B). In qualitative image analysis, 2 readers also scored the homogeneity of fat suppression as follows: reader 1, 4 and reader 2, 4.

to be spectrally selective only for fat magnetization. As the pulses pass through the fat null point (when the fat signal is zero), a conventional magnetic resonance sequence is initiated. Unlike CHESS, however, this technique does not need an accurate 90 degrees flip angle that depends on B1 homogeneity before the spoiler pulse. Additionally, SPAIR uses a frequency and phase-modulated pulse, called an adiabatic inversion pulse, that is specifically designed to be insensitive to B1 homogeneity.[22] Previous reports suggested that the implementation of SPAIR in 3T MRI will result in more homogeneous fat saturation than was possible with previous fat suppression techniques.[18,19]

The mDixon technique is a variant of Dixon imaging. In its original implementation, the Dixon method resulted in the acquisition of 1 image with water and fat signals in-phase and another image with water and fat signals 180° out-of-phase. Simple summation and subtraction of the 2 images was shown to yield a water-only image and a fat-only image, respectively. Although the original Dixon technique is not sensitive to B1 homogeneity, like the CHESS technique, it also relies on the water/fat chemical shift difference. It is also sensitive to B0 homogeneity, and the acquisition time is usually longer, especially at low-magnetic field MRI because this technique relies on the generation of 2 different images.[27–29] Without proper phase correction, the Dixon methods results in incomplete water and fat separation. These phase corrections were initially developed for the three-point Dixon technique. Previous reports suggested that the iterative least-squares decomposition method (the iterative decomposition of water and fat with echo asymmetry and least-squares estimation; IDEAL, GE

FIGURE 3. A 92-year-old man weighing 50 kg was suspected of having prostate carcinoma because of an elevated prostate-specific antigen level. He was underwent dynamic enhanced 3T MRI of the prostate with SPAIR technique. The signal intensity of subcutaneous fat (arrows) and perirectal fat (arrowheads) are not suppressed by SPAIR technique in first phase image and second phase image (A and B). In qualitative image analysis, 2 readers also scored the homogeneity of fat suppression as follows: reader 1, 2 and reader 2, 2. Therefore, the margin of rectal is unclear.

Healthcare) offered uniform fat-water separation.[30] The disadvantage of this technique is the long acquisition time needed for the 3-point acquisition. To solve this problem, many of the phase-correction algorithms were extended to allow a two-point Dixon technique, such as phase unwrapping by means of polynomial fitting, region growing, or solving of the Poisson equations.[31,32] The mDixon technique is the extension of this iterative least-squares decomposition of the three-point to the two-point Dixon technique.[23] Its use yielded in-phase, opposed phase, water, fat images from complex water and fat images with phase-correction from the flexible dual-echo acquisition, in addition to a reduction of scan times because of the shortened echo times.

Two features of 3T MRI can explain the stronger homogeneous suppression of the fat signal and the higher image quality of the mDixon technique than the SPAIR technique although their scan times and special resolution are similar. First, the inhomogeneity of the magnetic field is larger on 3T-MRI than on 1.5T MRI.[9,33] The mDixon technique is insensitive to both B0 and B1 homogeneity because it does not need an accurate 90 degrees flip angle and includes phase corrections through postprocessing algorithms, data acquisition, or a combination of both.[34] Although the SPAIR technique is also insensitive to B1 homogeneity, it is relatively sensitive to B0 inhomogeneity.[35] The frequency selection of fat in the SPAIR technique requires a homogeneity of the B0 magnetic field that is substantially less than the chemical shift difference between water and fat (3.5 ppm) within the entire field of view. This is because, due to an inhomogeneous B0 field, the water–fat spectra shift in some locations, such that the SPAIR pulse will either not suppress fat or it will suppress water instead of fat. Second, phase cycling in 3T MRI is twice as fast as in 1.5T MRI; in other words, 3T MRI can acquire in-phase and opposed-phase echoes in half the time needed by 1.5T MRI.[33] Although the mDixon technique offers flexible echo times, it is difficult to perform phase correction using 2 images in similar phase cycles.[34] With 3T MRI, the phase cycle fluctuates quickly, with the possibility to obtain two images at entirely different cycle phases within a short time. Therefore, the scan parameters of mDixon are more flexible in 3T MRI than in 1.5T MRI, and the scan time is accordingly shortened. In agreement with our results in dynamic imaging of the prostate, a previous report on dynamic enhanced 3T MRI of the liver suggested that the mDixon technique could improve the homogeneity of fat suppression over that obtained with the SPAIR technique.[35]

Our study suggested that the fat suppression in mDixon protocol might be better than that in SPAIR protocol. We think that the mDixon protocol might be useful in determining the extracapsular invasion compared with SPAIR technique. We would compare the diagnosability of the extracapsular invasion between two protocols in the future study.

Our study had several limitations. First, although image quality was assessed subjectively and objectively, we did not take into account the diagnostic performance of the 2 protocols in the detection of prostate carcinoma. Second, we only performed quantitative image analysis of transition zone. However, we did not evaluate the transition zone in quantitative image analysis. Third, the small sample size of our study limited our ability to generalize the results. Fourth, slightly different sequence parameters, such as matrix size, were used in mDixon-eTHRIVE and SPAIR-eTHRIVE due to vendor-imposed restrictions in the sequences, which may have affected image quality. Fifth, mDixon group and SPAIR group were different sample. The reason was why the purpose of this study was to evaluate the image quality between mDixon group and SPAIR group in postcontrast MRI. Therefore, we did not scan the same sample with mDixon technique and SPAIR technique in precontrast phase. Fifth, we did not compare CHESS technique,

SPAIR and mDixon techniques in dynamic MRI. We would compare 3 fat suppression techniques in dynamic prostatic MRI in the future study. Additionally, we evaluated the fat suppression to measure the signal intensity of subcutaneous fat and perirectal fat instead of that of the periprostatic fat between mDixon protocol and SPAIR protocol. The reason was that we cannot measure the signal intensity of the periprostatic fat exactly for the rich vascularity in the periprostatic fat. Lastly, the mDixon technique requires a complex iterative calculation using a postprocessing method. Although the scan time of the mDixon technique is almost the same as that of the SPAIR technique, the reconstruction time of mDixon technique is about 10 times longer.

In conclusion, in dynamic contrast-enhanced MRI of the prostate, the mDixon technique provided a better homogeneity of fat suppression without degrade of image quality than obtained with the SPAIR technique.

REFERENCES

1. Fujiwara K, Isaka S, Shimazaki J. Magnetic resonance imaging in the diagnosis of prostatic carcinoma and benign hyperplasia. *Nihon Hinyokika Gakkai Zasshi*. 1989;80:1336–1342.

2. Aziza R, Soulié M, Escourrou G, et al. [Local staging of prostate carcinoma with phased array MR imaging: prospective study over 5 years]. J Radiol. 2002;83:39–44.

3. Heckl S, Pipkorn R, Waldeck W, et al. Intracellular visualization of prostate cancer using magnetic resonance imaging. *Cancer Res*. 2003;63: 4766–4772.

4. Gore JC, Emery EW, Orr JS, et al. Medical nuclear magnetic resonance imaging: I. Physical principles. *Invest Radiol*. 1981;16:269–274.

5. Yu JS, Chung JJ, Hong SW, et al. Prostate cancer: added value of subtraction dynamic imaging in 3T magnetic resonance imaging with a phased-array body coil. *Yonsei Med J*. 2008;49:765–774.

6. Kim CK, Park BK, Kim B. Localization of prostate cancer using 3T MRI: comparison of T2-weighted and dynamic contrast-enhanced imaging. *J Comput Assist Tomogr*. 2006;30:7–11.

7. Rouviere O, Hartman RP, Lyonnet D. Prostate MR imaging at high-field strength: evolution or revolution? *Eur Radiol*. 2006;16:276–284.

8. Frahm J, Haase A, Hanicke W, et al. Chemical shift selective MR imaging using a whole-body magnet. *Radiology*. 1985;156:441–444.

9. Franklin KM, Dale BM, Merkle EM. Improvement in B1-inhomogeneity artifacts in the abdomen at 3T MR imaging using a radiofrequency cushion. *J Magn Reson Imag*. 2008;27:1443–1447.

10. Bloch BN, Furman-Haran E, Helbich TH, et al. Prostate cancer: accurate determination of extracapsular extension with high-spatial-resolution dynamic contrast-enhanced and T2-weighted MR imaging—initial results. *Radiology*. 2007;245:176–185.

11. Padhani AR, Gapinski CJ, Macvicar DA, et al. Dynamic contrast enhanced MRI of prostate cancer: correlation with morphology and tumour stage, histological grade and PSA. *Clin Radiol*. 2000;55:99–109.

12. Weinreb JC, Barentsz JO, Choyke PL, et al. PI-RADS prostate imaging—reporting and data system: 2015, Version 2. *Eur Urol*. 2016;69: 16–40.

13. Tamler B, Sommer FG, Glover GH, et al. Prostatic MR imaging performed with the three-point Dixon technique. Work in progress. *Radiology*. 1991;179:43–47.

14. Parivar F, Rajanayagam V, Waluch V, et al. Endorectal surface coil MR imaging of prostatic carcinoma with the inversion-recovery sequence. *J Magn Reson Imag*. 1991;1:657–664.

15. Tempany CM, Zhou X, Zerhouni EA, et al. Staging of prostate cancer: results of Radiology Diagnostic Oncology Group project comparison of three MR imaging techniques. *Radiology*. 1994;192:47–54.

16. Mirowitz SA, Heiken JP, Brown JJ. Evaluation of fat saturation technique for T2-weighted endorectal coil MRI of the prostate. *Magn Reson Imaging*. 1994;12:743–747.

17. Duewell SH, Ceckler TL, Ong K, et al. Musculoskeletal MR imaging at 4 T and at 1.5 T: comparison of relaxation times and image contrast. *Radiology*. 1995;196:551–555.

18. Miyazaki M, Wheaton A, Kitane S. Enhanced fat suppression technique for breast imaging. *J Magn Reson Imag*. 2013;38:981–986.

19. Lauenstein TC, Sharma P, Hughes T, et al. Evaluation of optimized inversion-recovery fat-suppression techniques for T2-weighted abdominal MR imaging. *J Magn Reson Imaging*. 2008;27:1448–1454.

20. Li XH, Zhu J, Zhang XM, et al. Abdominal MRI at 3.0 T: LAVA-Flex compared with conventional fat suppression T1-weighted images. *J Magn Reson Imaging*. 2014;40:58–66.

21. Foo TK, Sawyer AM, Faulkner WH, et al. Inversion in the steady state: contrast optimization and reduced imaging time with fast three-dimensional inversion-recovery-prepared GRE pulse sequences. *Radiology*. 1994;191:85–90.

22. Tannus A, Garwood M. Adiabatic pulses. *NMR Biomed*. 1997;10:423–434.

23. Eggers H, Brendel B, Duijndam A, et al. Dual-echo Dixon imaging with flexible choice of echo times. *Magn Reson Med*. 2011;65:96–107.

24. Brown G, Macvicar DA, Ayton V, et al. The role of intravenous contrast enhancement in magnetic resonance imaging of prostatic carcinoma. *Clin Radiol*. 1995;50:601–606.

25. Bogner W, Gruber S, Pinker K, et al. Diffusion-weighted MR for differentiation of breast lesions at 3.0 T: how does selection of diffusion protocols affect diagnosis? *Radiology*. 2009;253:341–351.

26. Murtz P, Tsesarskiy M, Kowal A, et al. Diffusion-weighted magnetic resonance imaging of breast lesions: the influence of different fat-suppression techniques on quantitative measurements and their reproducibility. *Eur Radiol*. 2014;24:2540–2551.

27. Ohno S, Togami I, Kitayama T, et al. Study of gradient echo (GRE) Dixon image using low-field MRI scanner for examination of metastatic bone marrow tumors: comparison of double and single echo sequences. *Nihon Hoshasen Gijutsu Gakkai zasshi*. 2002;58:1377–1382.

28. Ozaki T, Sugihara S, Hamada M, et al. Magnetic resonance chemical shift imaging in bone and soft tissue tumours. *Int Orthop*. 1997;21:9–13.

29. Bredella MA, Losasso C, Moelleken SC, et al. Three-point Dixon chemical-shift imaging for evaluating articular cartilage defects in the knee joint on a low-field-strength open magnet. *AJR Am J Roentgenol*. 2001;177:1371–1375.

30. Reeder SB, Pineda AR, Wen Z, et al. Iterative decomposition of water and fat with echo asymmetry and least-squares estimation (IDEAL): application with fast spin-echo imaging. *Magn Reson Med*. 2005;54:636–644.

31. Coombs BD, Szumowski J, Coshow W. Two-point Dixon technique for water-fat signal decomposition with B0 inhomogeneity correction. *Magn Reson Med*. 1997;38:884–889.

32. Skinner TE, Glover GH. An extended two-point Dixon algorithm for calculating separate water, fat, and B0 images. *Magn Reson Med*. 1997;37:628–630.

33. Dietrich O, Reiser MF, Schoenberg SO. Artifacts in 3-T MRI: physical background and reduction strategies. *Eur J Radiol*. 2008;65:29–35.

34. Ma J. Dixon techniques for water and fat imaging. *J Magn Reson Imaging*. 2008;28:543–558.

35. Lee MH, Kim YK, Park MJ, et al. Gadoxetic acid-enhanced fat suppressed three-dimensional T1-weighted MRI using a multiecho dixon technique at 3 tesla: emphasis on image quality and hepatocellular carcinoma detection. *J Magn Reson Imaging*. 2013;38:401–410.